Crammer-Rao Lower Bound of Vehicular Position & Orientation using a Lens-based MIMO in the Cooperative Vehicle-to-Vehicle (V2V) Systems

Joohyun Jo
Department of Electrical and Electronic Engineering
Yonsei University
Seoul, South Korea
joohyun_jo@yonsei.ac.kr

Dong Ku Kim
Department of Electrical and Electronic Engineering
Yonsei University
Seoul, South Korea
dkkim@yonsei.ac.kr

***Abstract*—We derive theoretical limits of estimation on the position and orientation of vehicles equipped with lens based arrays in cooperative Vehicle to Vehicle (V2V) scenario. Then, we analyze and compare its performance with conventional linear array. We determine a received signal of a lens-embedded antenna array and V2V geometric model, with which we next derive the Cramér-Rao lower bound (CRLB) on position and orientation estimation. We verify that a lens-based multiple-input multiple-output (MIMO) outperforms a conventional uniform linear array (ULA) in a certain constraint of a lens's structure.**

***Index Terms*—Position and Orientation, Crammer-Rao lower bound, Lens antenna, Cooperative Localization.**

I. Introduction

High accurate position is one of the key requirements to most of Day-2 advanced driving services, such as location-aware communications for the 5G vehicle-to-everything (V2X) networks at the street intersection depicted in the 3rd Generation Partnership Project (3GPP) Rel-16 [1]–[3]. Particularly, the 5G Automotive Association (5GAA) reported a highly accurate localization requirement as one of key indicators for the autonomous vertical industries [4]. Furthermore, the orientation of vehicles helps an efficient prediction of vehicle's maneuvering to support autonomous driving vehicles to make quicker, safer by the planned movements of surrounding vehicles [5]. To fulfill these demands, the cooperative vehicle-to-vehicle (V2V) based on the millimeter-wave (mmWave) multiple-input-multiple-output (MIMO) has been proposed [6]. The mmWave has a characteristic of propagating in LoS path with little reflection and scattering, enabling high precision positioning. However, it costs a great deal of complexity and energy consumption to overcome higher path loss compared to current 5.9GHz ITS frequency band. To deal with its problem, a lens antenna array have been introduced and studied in the vehicular applications [7], [8].

In NR-V2X, several positioning solutions in radio access network (RAN) are standardized to meet the requirements of V2X services, in which there are infrastructures such as a base-station, location server and road-side-unit [9]. In these solutions, the infra determine vehicular locations in terms of the measurement of angles and distance from vehicles.

Furthermore, the sidelink assisted positioning schemes in dense V2V networks will help meet the accurate localization requirement, which is under discussion in 3GPP Rel-18 work item [10]. The investigation on the error bound and its estimation schemes of localization has been also conducted in a conventional uniform linear array (ULA) [11], [12].

In this paper, we analyze and compare the cooperative V2V positioning performance by introducing a lens-based array that can guarantee the performance with low complexity [13]. First, we determine a V2V model for a cooperative position and orientation estimation based on the Cramér-Rao lower bound (CRLB) of an AoA with which we derive the CRLB for position and orientation. We then compare the bounds with and without lens, and demonstrate that the localization performance with the lens MIMO is better than a conventional ULA.

Notation: For a matrix $\mathbf{A}$, $\mathbf{A}^T$, $\mathbf{A}^{-1}$, and $\mathbf{tr}(\mathbf{A})$ are the transpose, inverse, and trace operation respectively. $\mathbb{E}$ is expectation of a random variable.

II. System model

In this section, we describe the received signal of lens MIMO systems in terms of wave optics on the geometrical model for cooperative V2V positioning and orientation estimation. Location of the k-th vehicle is denoted by the position $\mathbf{p}_k = [x_k, y_k]^T \in \mathbb{R}^2$ and the orientation angle of the receiver's antenna array $\omega_k \in [0, 2\pi)$.

A. Signal Model

We consider a lens-based mmWave MIMO system where a receiver equipped with N_r received antenna elements. Considering each V2V links for the k-th vehicle, the received signal

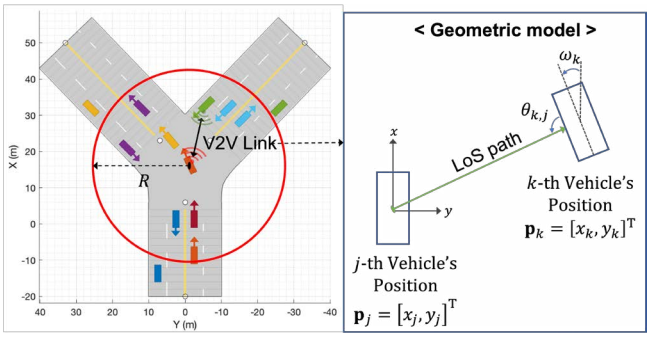

Fig. 1. V2V scenario for position & orientation estimation

at the n_r-th antenna element can be defined by an AoA $\theta_{k,j}$ from the j-th vehicle in a communication radius [14].

$$[\mathbf{y}_{k,j}]_{n_r} = \frac{L}{\sqrt{x}}\text{sinc}\left[\frac{L}{\lambda}\left\{\sin\theta_{n_r} - \sin\theta_{k,j}\right\}\right] e^{-j2\pi x/\lambda} + [\mathbf{n}]_{n_r}, \tag{1}$$

where L, x and λ are a lens aperture, focal length and a wave length of operating frequency, respectively. The antenna elements are placed on a focal region represented by $\theta_{n_r} \in \left\{\sin\left(\frac{\lambda}{L}n_r\right) : n_r = -\frac{N_r-1}{2}, \ldots, \frac{N_r-1}{2}\right\}$, and $\mathbf{n} \in \mathbb{C}^{N_r \times 1}$ is the additive white Gaussian noise (AWGN) vector following the distribution of $\mathcal{CN}(0, \sigma_n^2)$.

It is evident that AoA affect only the amplitude and phase term at antenna array depends only on the distance from the lens to antenna array.

B. Geometric Model

We consider a use case of street intersection in V2V networks where a set of vehicles N_v vehicles $\mathcal{V} = \{1, \ldots, N_v\}$ equipped with mmWave lens MIMO array are approaching and crossing the intersection. Their communication range is assumed to be R on two dimensional space as shown in Fig. 1. Then, the measured AoA from vehicle j to k can be represented as function of geometric structure in Fig. 1.

$$\theta_{k,j} = g(\mathbf{p}_k, \mathbf{p}_j, \omega_k) + n_B(\theta_{k,j}), \tag{2}$$

where $\theta_{k,j}$ is the measured AoA, which is tilted by ω_k, at the k-th node from the j-th node where $j \in \mathcal{V}$, the function $g(\mathbf{p}_k, \mathbf{p}_j, \omega_k)$ depend on the measurement model with respect to vehicle's positions and orientations, $\mathbf{p}_k$ and $\mathbf{p}_j$ are true locations, $n_B(\theta_{k,j})$ is a Gaussian noise with zero mean and variance $\sigma^2_{B_{k,j}}$ whose lower bound is CRLB of the AoA $\theta_{k,j}$. In the case of conventional ULA and lens MIMO systems, its can be readily derived as follows [14],

$$CRLB_{ULA}(\theta) = \frac{6\sigma_n^2}{N_R(N_R^2-1)d^2\cos^2\theta}, \tag{3}$$

$$CRLB_{Lens}(\theta) = \frac{\sigma_n^2}{2}\sum_{n_r}\mathbf{a}^2_{n_r}(\theta)\Big/\left[\left\{\sum_{n_r}\mathbf{a}^2_{n_r}(\theta)\right\}\right.$$
$$\left.\sum_{n_r}\left\{\frac{\partial}{\partial\theta}\mathbf{a}_{n_r}(\theta)\right\} - \left\{\sum_{n_r}\mathbf{a}_{n_r}(\theta)\frac{\partial}{\delta\partial}\mathbf{a}_{n_r}(\theta)\right\}^2\right], \tag{4}$$

where d is an antenna spacing of ULA, and $\mathbf{a}_{n_r}(\theta) = \frac{L}{\sqrt{x}}\text{sinc}\left[\frac{L}{\lambda}\left\{\sin\theta_{n_r} - \sin\theta\right\}\right]$ is a steering vector corresponding to the amplitude of the received signal in (1). These bounds are considered to be the variance of AoA model's noise in (2).

Considering AoA measurement, $g(.)$ is modeled as

$$g(\mathbf{p}_k, \mathbf{p}_j, \omega_k) = \tan^{-1}\left(\frac{y_j - y_k}{x_j - x_k}\right) - \omega_k. \tag{5}$$

We assume that all vehicles communicate with each others with LoS path in mmWave band. For AoA in the LoS condition, each measured AoAs can be modeled as independent and identically distributed (i.i.d.) zero mean Guassian random variable with variance $\sigma^2_{B_{k,j}}$. Following this assumption, the joint probability of the AoAs $\boldsymbol{\theta}$, defined by a set of $\theta_{k,j}\ \forall j \in \mathcal{V}$, can expressed as

$$f(\boldsymbol{\theta}|\mathbf{p}_k, \omega_k) = \prod_{j\in\mathcal{V}} f(\theta_{k,j}|\mathbf{p}_k, \mathbf{p}_j, \omega_k)$$
$$= \prod_{j\in\mathcal{V}} \frac{1}{\sqrt{2\pi\sigma^2_{B_{k,j}}}} exp\left(-\frac{(\theta_{k,j} - \alpha_{k,j})^2}{2\sigma^2_{B_{k,j}}}\right), \tag{6}$$

where $\boldsymbol{\theta}$ is a vector consisting of all AoA measurement, $\mathcal{V}$ is the set of vehicles within the communication radius of k-th vehicle, $\alpha_{k,j}$ is an abbreviated form of the $g(\mathbf{p}_k, \mathbf{p}_j, \omega_k)$ in (3). The concept of AoA measurement at kth vehicle is depicted in Fig. 1. We suppose that orientations of neighbors in the communication range are known but arbitrary, then each vehicles can measure the tilted AoA from the set of neighbors.

III. THEORETICAL BOUND

In this section, we explore the CRLB for positioning and orientation of lens based-array and conventional linear array.

A. CRLB Derivation for Position & Orientation

In order to investigate lower bound of position and orientation accuracy, we define the vector consisting of unknown location parameters

$$\boldsymbol{\eta} = \left[\boldsymbol{\eta}_0^T, \ldots, \boldsymbol{\eta}_{N_v}^T\right]^T \in \mathbb{R}^{3N_v \times 1}, \tag{7}$$

in which $\boldsymbol{\eta}_k^T$ consists of the unknown parameters (position $\mathbf{p}_k$ and orientation ω_k) for the k-th vehicle. Defining $\hat{\boldsymbol{\eta}}$ as the unbiased estimator of $\boldsymbol{\eta}$, the error variance satisfy inequality as [15],

$$\mathbb{E}_{\boldsymbol{\theta}|\boldsymbol{\eta}}[(\boldsymbol{\eta} - \hat{\boldsymbol{\eta}})(\boldsymbol{\eta} - \hat{\boldsymbol{\eta}})^T] \geq F^{-1}(\boldsymbol{\eta}), \tag{8}$$

where $\mathbb{E}_{\boldsymbol{\theta}|\boldsymbol{\eta}}[.]$ denotes the expectation parameterized by unknown parameters, and the Fisher information matrix (FIM) $F(\boldsymbol{\eta})$ is defined by

$$F(\boldsymbol{\eta}) = -\mathbb{E}_{\boldsymbol{\theta}|\boldsymbol{\eta}}\left[\frac{\partial^2 \ln f(\boldsymbol{\theta}|\boldsymbol{\eta})}{\partial \boldsymbol{\eta} \partial \boldsymbol{\eta}^T}\right]. \tag{9}$$

The $3N_v \times 3N_v$ FIM $F(\boldsymbol{\eta})$ can be constructed in blocks as the $N_v \times N_v$ sub-block matrix for unknown parameters, it is formed as

$$F(\boldsymbol{\eta}) = \begin{bmatrix} F_{\mathbf{xx}} & F_{\mathbf{xy}} & F_{\mathbf{xw}} \\ F_{\mathbf{yx}} & F_{\mathbf{yy}} & F_{\mathbf{yw}} \\ F_{\mathbf{wx}} & F_{\mathbf{wy}} & F_{\mathbf{ww}} \end{bmatrix}. \tag{10}$$

The elements of $N_v \times N_v$ $F_{\mathbf{xx}}$ matrix can be obtained by the geometric model in (5) as follows,

$$[F_{\mathbf{xx}}]_{i,j} = \begin{cases} \sum_{j \in \mathcal{V}} \frac{1}{\sqrt{2\pi\sigma^2_{B_{k,j}}}} \frac{1}{\sigma^2_{B_{k,j}}} \frac{(y_j - y_k)^2}{d^4_{j,k}}, & \text{for } i = j \\ 0, & \text{otherwise,} \end{cases} \tag{11}$$

where $d_{j,k}$ is a distance of vehicles from k to j. In detail, it is proved in Appendix A.

The diagonal term of each sub-matrix can be derived in the same way as:

$$[F_{yy}]_{i,i} = \sum_{j \in \mathcal{V}} \frac{1}{\sqrt{2\pi\sigma^2_{B_{k,j}}}} \frac{1}{\sigma^2_{B_{k,j}}} \frac{(x_j - x_k)^2}{d^4_{j,k}}, \tag{12}$$

$$[F_{xy}]_{i,i} = [F_{yx}]_{i,i} = \sum_{j \in \mathcal{V}} \frac{1}{\sqrt{2\pi\sigma^2_{B_{k,j}}}} \frac{1}{\sigma^2_{B_{k,j}}} \frac{(x_j - x_k)(y_j - y_k)}{d^4_{j,k}}, \tag{13}$$

$$[F_{xw}]_{i,i} = [F_{wx}]_{i,i} = -\sum_{j \in \mathcal{V}} \frac{1}{\sqrt{2\pi\sigma^2_{B_{k,j}}}} \frac{1}{\sigma^2_{B_{k,j}}} \frac{(y_j - y_k)}{d^2_{j,k}}, \tag{14}$$

$$[F_{yw}]_{i,i} = [F_{wy}]_{i,i} = -\sum_{j \in \mathcal{V}} \frac{1}{\sqrt{2\pi\sigma^2_{B_{k,j}}}} \frac{1}{\sigma^2_{B_{k,j}}} \frac{(x_j - x_k)}{d^2_{j,k}}, \tag{15}$$

$$[F_{ww}]_{i,i} = \sum_{j \in \mathcal{V}} \frac{1}{\sqrt{2\pi\sigma^2_{B_{k,j}}}} \frac{1}{\sigma^2_{B_{k,j}}}, \tag{16}$$

and the rest entries (i.e. off-diagonal term of each sub-block) are zero.

By exploiting the derived FIM, we can obtain the vehicle's position and rotation error bound, defined by B_p and B_o, as follows,

$$\text{PEB}_p \geq \sqrt{\mathbf{tr}\left\{[F(\boldsymbol{\eta})^{-1}]_{1:2N_v,1:2N_v}\right\}}, \tag{17}$$

$$\text{PEB}_o \geq \sqrt{\mathbf{tr}\left\{[F(\boldsymbol{\eta}^{-1})]_{2N_v+1:\text{end},2N_v+1:\text{end}}\right\}}, \tag{18}$$

where the operation $[.]_{i:j,i:j}$ denotes the selection of sub-matrix from i-th to j-th entry.

B. Analysis of CRLB

As the derived FIM, elements are attributed the AoA error variance $\sigma^2_{B_{k,j}}$. Assuming the same signal-to-noise ratio (SNR) for both ULA and lens array, a smaller CRLB of AoA (*i.e.* AoA error variance $\sigma^2_{B_{k,j}}$) assures better position and orientation accuracy. So, we compare the CRLB of AoA with and without lens. The CRLB of lens-based AoA estimation cannot be directly compared to ULA because of the term of squared amplitude in (4).

For comparison of CRLB with and without lens, we set all antenna elements are on the focal region, i.e. $x = f$. Then, to derive a derivative of the amplitude, let define μ_1 and μ_2 as

$$\boldsymbol{\mu}_1 = \text{sinc}\left(\frac{Ldn_r}{f\lambda} - \frac{L}{\lambda}\sin\theta\right), \tag{19}$$

$$\boldsymbol{\mu}_2 = \frac{\partial}{\partial\theta}\text{sinc}\left(\frac{Ldn_r}{f\lambda} - \frac{L}{\lambda}\sin\theta\right). \tag{20}$$

To represent CRLB of AoA with lens in (4), let denote that $\mathbf{a}_{n_r} = \frac{L}{\sqrt{f}}\boldsymbol{\mu}_1$ and $\frac{\partial}{\partial\theta}\mathbf{a}_{n_r} = \frac{L^2}{\lambda\sqrt{f}}\cos\theta\boldsymbol{\mu}_2$. Then, the CRLB can be represented by

$$CRLB_{Lens}(\theta) = \frac{f\lambda^2\sigma_n^2}{2p^2L^4\cos\theta^2} \cdot \frac{\boldsymbol{\mu}_1^T\boldsymbol{\mu}_1}{[\boldsymbol{\mu}_1^T\boldsymbol{\mu}_1][\boldsymbol{\mu}_2^T\boldsymbol{\mu}_2] - [\boldsymbol{\mu}_1^T\boldsymbol{\mu}_2]}. \tag{21}$$

For comparison between bounds, we assume that antenna spacing is the critical sampling of the sinc function that is represented by $\theta \in \left\{\sin^{-1}\left(\frac{\lambda}{L}n_r\right) : n_r = -\frac{N_r-1}{2}, \ldots, \frac{N_r-1}{2}\right\}$, $d = \frac{f}{L}\lambda$ given by in [16]. In other words, the lens antenna array works like a discrete fourier transform (DFT) beamformer. Then,

$$\begin{aligned} \boldsymbol{\mu}_1^T\boldsymbol{\mu}_1 &= 1, \\ \boldsymbol{\mu}_1^T\boldsymbol{\mu}_2 &= 0, \\ 1 \leq \boldsymbol{\mu}_2^T\boldsymbol{\mu}_2 &\leq 2. \end{aligned} \tag{22}$$

By these inequalities, the CRLB of lens can be simplified as follows,

$$CRLB_{Lens}(\theta) = \frac{f\lambda^2\sigma_n^2}{2p^2L^4\cos\theta^2} \cdot \frac{1}{[\boldsymbol{\mu}_2^T\boldsymbol{\mu}_2]}. \tag{23}$$

Let assume that $CRLB_{Lens} \leq CRLB_{ULA}$, then the condition for comparison between bounds with and without lens is readily derived.

$$CRLB_{Lens} < CRLB_{ULA} \; where \, f < \frac{12L^3}{(2L+1)(L+1)\lambda^4}. \tag{24}$$

Proof: See Appendix B.

Suppose that the focal length is set to the minimum $f = \frac{L}{2}$ to satisfy preceding conditions [17], and substitute the minimum focal length into the condition in (24), it then becomes

$$\frac{12L^3}{(2L+1)(L+1)\lambda^4} > \frac{L}{2}. \tag{25}$$

The above inequality (25) is always satisfied for any L. To describe its satisfied region for L, Fig. 2 verifies that the left-hand side is always bigger then right-hand side.

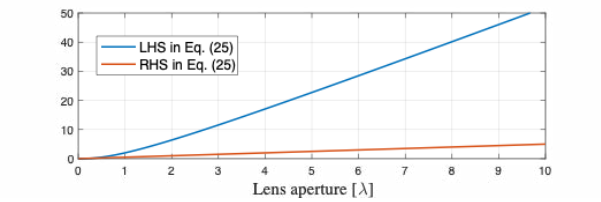

Fig. 2. Conditions as a function of lens aperture

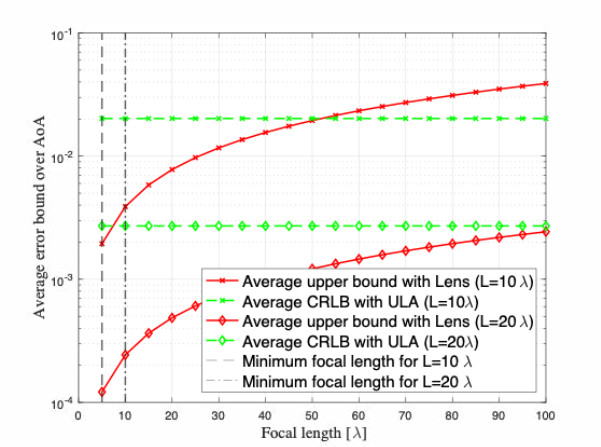

Fig. 3. Error bound as a function of focal length

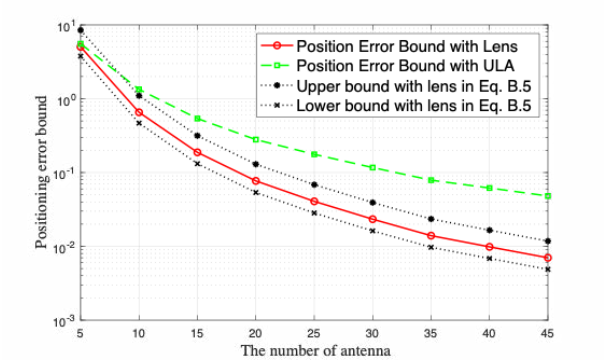

(a) Position

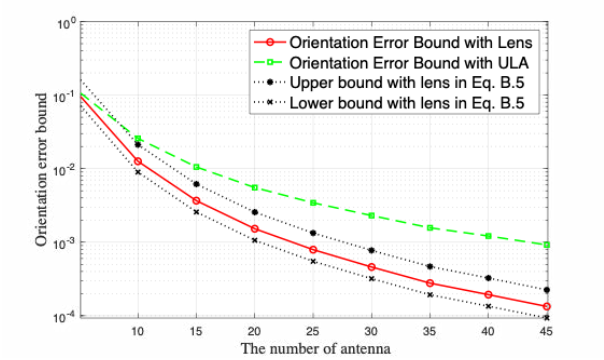

(b) Orientation

Fig. 4. Error bound as a function of the number of antenna

Even if the focal length satisfies the condition of the minimum $f \geq \frac{L}{2}$, the performance of the lens may deteriorate if only f is increased while the aperture L is fixed. In Fig. 3, we compare the derived upper bound with lens in (B.5) and CRLB with a conventional ULA with fixed apertures. For a fair comparison, we set the number of antennas to $2L+1$ for both with and without lens in which each antenna spacing is f/L for lens and $\lambda/2$ for ULA, where SNR is set to be 5dB. Each Y-axis and X-axis in Fig. 3 represents averaged bound over AoA $\theta \in [-\frac{\pi}{2}, \frac{\pi}{2}]$ and focal length f. In each cases, the lens has a dominant performance at the minimum focal length, and it has better performance until the focal length is about five times the lens aperture. Given a value of L, however, its performance shows the degradation as f increases more than $L/2$ since the amplitude gain at the antenna array gets smaller in (4) and distance in-between antennas gets wider than critical sampling spacing f/L. Therefore, it is essential to design a focal length suitable for a aperture and antenna array to enhance the localization performance.

The analysis confirmed that the condition for a dominant estimation performance of the lens antenna, and the performance for positioning and orientation estimation is superior to the conventional ULA.

IV. NUMERICAL RESULTS

In this section, we explain a cooperative V2V scenario for simulations, and evaluate the derived CRLB of localization parameters.

A. Parameter setup

The simulation setup consist of the street intersection with a lane width 5m and length 50m depicted in Fig. 1. Vehicles are dropped on the road as the Poisson process, and each vehicles is tilted by ω_k following the uniform distribution $[0, 2\pi)$. For the path loss of each LoS link, denoted by ρ_0, is adapted by geometric statistics [18].

$$\frac{1}{\rho_0} = \zeta^2(d_{k,j}) \left(\frac{\lambda}{4\pi d_{k,j}} \right)^2, \tag{26}$$

where $\zeta^2(d_{k,j})$ is the atmospheric attenuation over distance $d_{k,j}$. The lens aperture is equal to the size of ULA, and the antenna spacing of each cases is the critical sampling f/L for lens and $\lambda/2$ for ULA. The number of antenna elements is $2L+1$ for both cases. We assume that each of vehicles can estimate AoAs from vehicles in a communication radius $R = 30$.

B. Results of CRLB

First, we compare CRLB bounds of the localization parameters (position $\mathbf{p}$ and orientation ω) with and without lens according to the number of antenna, where SNR and focal length are set up to 5dB and 40λ in Fig. 4. The X-axis can be represented by the lens aperture $W = [0, 80\lambda]$, which is the feasible region for the condition of the minimum focal length

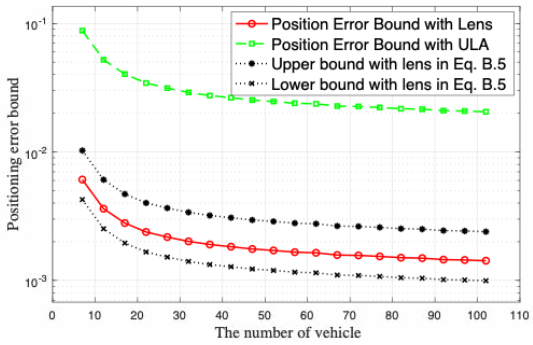

(a) Position

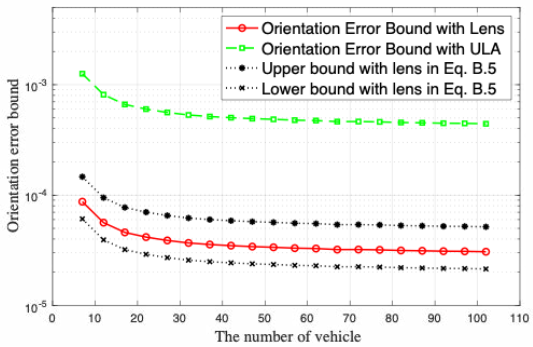

(b) Orientation

Fig. 5. Error bound as a function of the number of vehicle

in (25). We verify the localization accuracy is proportional to the number of antennas. It is also noticed that the upper bound of a lens-based CRLB starts to get smaller than a conventional linear array when the number of antennas is around 10. In more than the antenna elements, the performance of the lens is better than ULA, and the difference is more noticeable as the number of antennas increases. In other words, if the lens size is sufficient for a given focal length, the performance of lens antenna is guaranteed.

In Fig. 5, we compare bounds for increasing number of vehicles. The number of antennas and SNR are fixed by $N_r = 121$ and SNR=0dB. Through the results, we confirm that the performance of positioning with orientation is proportional to the number of vehicles, but there is a limitation. The performance of both parameters with the lens antenna array is always superior to the conventional ULA due to the larger lens aperture of many antenna elements. The difference in performance is verified through the derived bound proportional to the aperture in (B.5). The performance of the lens is also in-between bounds in (B.5), it clarifies the analysis of CRLB in the section III-B.

V. CONCLUSION

In this paper, we have derived the theoretical limit of localization for cooperative V2V scenario where vehicles are equipped with a lens antenna array, and compared it with a conventional ULA. We confirmed that the bounds of position and orientation are affected by CRLB of AoA, and proved that the performance of positioning with lens is better than a conventional ULA under certain condition. The simulation verifies that the localization accuracy gets enhanced as the number of antennas and vehicles increases, and shows that the performance of lens antenna outperforms than ULA. For future works, we will research an algorithm satisfying the bound of localization with orientation in the lens MIMO systems.

ACKNOWLEDGMENT

This research was a part of the project titled 'The advancement of smart aids to navigation facilities (20210636)', funded by the Ministry of Oceans and Fisheries, Korea.

VI. APPENDIX

A. Appendix A

This section focuses on evaluating the element of Fisher Information Matrix. the $[F_{\mathbf{xx}}]_{i,j}$ is written as

$$[F_{\mathbf{xx}}]_{i,j} = \mathbb{E}\left[\frac{\partial \ln \mathbf{f}(\boldsymbol{\theta}|\boldsymbol{\eta})}{\partial x_i}\frac{\partial \ln \mathbf{f}(\boldsymbol{\theta}|\boldsymbol{\eta})}{\partial x_j}\right]. \tag{A.1}$$

Note that $\theta_{k,j}$ is independent of $\theta_{k,i}$ when $i \neq j$ by the mmWave assumption, then entries become to zero for $i \neq j$. The twice differentiation of $\mathbf{f}(\boldsymbol{\theta}|\boldsymbol{\eta})$ with respect to x_i and x_j is a exponential family, then we have,

$$[F_{\mathbf{xx}}]_{i,j} = \begin{cases} \sum_{j\in\mathcal{V}} \frac{\partial^2 \ln \mathbf{f}(\theta_{k,j}|\mathbf{p},\omega)}{\partial^2 x_k^2}, & \text{for } i = j \\ 0, & \text{otherwise.} \end{cases} \tag{A.2}$$

Considering the second derivative, we can derive the diagonal entry of FIM as follows,

$$\frac{\partial^2 \ln \mathbf{f}(\theta_{k,j}|\mathbf{p}_k, \mathbf{p}_j, \omega_k)}{\partial x_k^2} \tag{A.3}$$

$$= \frac{1}{\sqrt{2\pi\sigma^2_{B_{k,j}}}}\frac{\partial}{\partial x_k}\left[\frac{\partial}{\partial x_k}\left(-\frac{(\theta_{k,j}-\alpha_{k,j})^2}{2\sigma^2_{B_{k,j}}}\right)\right] \tag{A.4}$$

$$= \frac{1}{\sqrt{2\pi\sigma^2_{B_{k,j}}}}\frac{\partial}{\partial x_k}\left[\left(\frac{(\theta_{k,j}-\alpha_{k,j})}{\sigma^2_{B_{k,j}}}\right)\frac{\partial \alpha_{k,j}}{\partial x_k}\right] \tag{A.5}$$

$$= \frac{1}{\sqrt{2\pi\sigma^2_{B_{k,j}}}}\frac{\partial}{\partial x_k}\left[\left(\frac{(\theta_{k,j}-\alpha_{k,j})}{\sigma^2_{B_{k,j}}}\right)\frac{(y_j-y_k)}{d^2_{j,k}}\right] \tag{A.6}$$

$$= \mathbf{A}\left[-\frac{(y_j-y_k)^2}{d^4_{j,k}} + (\theta_{k,j}-\alpha_{k,j})\frac{\partial}{\partial x_k}\frac{(y_j-y_k)}{d^2_{j,k}}\right], \tag{A.7}$$

where $\mathbf{A} = \frac{1}{\sigma^2_{B_{k,j}}\sqrt{2\pi\sigma^2_{B_{k,j}}}}$ is the constant term. In (A.5), the derivative of the geometric form $\alpha_{k,j}$ is given by

$$\begin{aligned}\frac{\partial \alpha_{k,j}}{\partial x_k} &= \frac{\partial}{\partial x_k}\left(\tan^{-1}\left(\frac{y_j-y_k}{x_j-x_k}\right)-\omega_k\right) \\ &= \frac{y_j-y_k}{(y_j-y_k)^2+(x_j-x_k)^2} = \frac{y_j-y_k}{d^2_{j,k}}.\end{aligned} \tag{A.8}$$

Since $\mathbb{E}[\theta_{k,j}] = \alpha_{k,j}$, we have the k-th diagonal entry by substituting (A.7) into (A.1).

$$F_{\mathbf{xx}}(k,k) = \frac{1}{\sqrt{2\pi\sigma_{k,j}^2}} \frac{1}{\sigma_{k,j}^2} \frac{(y_j - y_k)^2}{d_{j,k}^4}. \tag{A.9}$$

This completes the proof of (11).

B. Appendix B

The first derivative of $sinc$ function can be represented as

$$\frac{\delta}{\delta x}\left(\frac{\sin \pi x}{\pi x}\right) = \begin{cases} 0, & \text{for } x = 0 \\ \frac{\pi x \cos(\pi x) - \sin(\pi x)}{\pi x^2}, & \text{otherwise.} \end{cases} \tag{B.1}$$

Suppose $x = Z$, where $Z \in \mathbb{Z}$, arbitrary integer. Then, $\sin \pi Z = 0$ and

$$\frac{\delta}{\delta x}\left(\frac{\sin \pi x}{\pi x}\right)|_{x=Z} = \begin{cases} 0, & \text{for } Z = 0 \\ \frac{1}{Z}, & \text{Z is odd} \\ -\frac{1}{Z}, & \text{Z is even.} \end{cases} \tag{B.2}$$

Then, the upper and lower bound of $\boldsymbol{\mu}_2^T \boldsymbol{\mu}_2$ is simply derived as follows,

$$\sum_{\ell=1}^{\frac{N_r-1}{2}} \frac{1}{\ell^2} < 1 + \sum_{\ell=1}^{\frac{N_r-1}{2}} \frac{1}{\ell(\ell-1)} = 2 - \frac{2}{N_r - 1} < 2, \tag{B.3}$$

$$\mu_2^T \mu_2 \geq \sum_{\ell=1}^{N_r} \frac{1}{\ell^2} \geq 1. \tag{B.4}$$

By substituting above inequalities into (23), the bound of CRLB can be determined, and we can readily compare bounds with and without lens.

$$\frac{f\lambda^2\sigma_n^2}{4L^4\cos^2\theta} < CRLB_{lens}(\theta) \leq \frac{f\lambda^2\sigma_n^2}{2L^4\cos^2\theta}. \tag{B.5}$$

This completes the proof of (24).

REFERENCES

[1] S. Dwivedi, R. Shreevastav, F. Munier, J. Nygren, I. Siomina, Y. Lyazidi, D. Shrestha, G. Lindmark, P. Ernström, E. Stare *et al.*, "Positioning in 5g networks," *IEEE Communications Magazine*, vol. 59, no. 11, pp. 38–44, 2021.

[2] H. Bagheri, M. Noor-A-Rahim, Z. Liu, H. Lee, D. Pesch, K. Moessner, and P. Xiao, "5G NR-V2X: Toward Connected and Cooperative Autonomous Driving," *IEEE Communications Standards Magazine*, vol. 5, no. 1, pp. 48–54, 2021.

[3] 3GPP TR 22.872, "Study on positioning use cases," 2018.

[4] 5GAA Technical Report, "System Architecture and Solution Development; High-Accuracy Positioning for C-V2X," 2021.

[5] M. H. C. Garcia, A. Molina-Galan, M. Boban, J. Gozalvez, B. Coll-Perales, T. Şahin, and A. Kousaridas, "A tutorial on 5g nr v2x communications," *IEEE Communications Surveys Tutorials*, vol. 23, no. 3, pp. 1972–2026, 2021.

[6] F. J. Martin-Vega, M. C. Aguayo-Torres, G. Gomez, J. T. Entrambasaguas, and T. Q. Duong, "Key technologies, modeling approaches, and challenges for millimeter-wave vehicular communications," *IEEE Communications Magazine*, vol. 56, no. 10, pp. 28–35, 2018.

[7] Y. Zeng, R. Zhang, and Z. N. Chen, "Electromagnetic Lens-Focusing Antenna Enabled Massive MIMO: Performance Improvement and Cost Reduction," *IEEE Journal on Selected Areas in Communications*, vol. 32, no. 6, pp. 1194–1206, 2014.

[8] F. Dong, W. Wang, Z. Huang, and P. Huang, "High-resolution angle-of-arrival and channel estimation for mmwave massive mimo systems with lens antenna array," *IEEE Transactions on Vehicular Technology*, vol. 69, no. 11, pp. 12 963–12 973, 2020.

[9] Q. Liu, P. Liang, J. Xia, T. Wang, M. Song, X. Xu, J. Zhang, Y. Fan, and L. Liu, "A highly accurate positioning solution for c-v2x systems," *Sensors*, vol. 21, no. 4, p. 1175, 2021.

[10] M. Harounabadi, D. M. Soleymani, S. Bhadauria, M. Leyh, and E. Roth-Mandutz, "V2x in 3gpp standardization: Nr sidelink in release-16 and beyond," *IEEE Communications Standards Magazine*, vol. 5, no. 1, pp. 12–21, 2021.

[11] Z. Abu-Shaban, X. Zhou, T. Abhayapala, G. Seco-Granados, and H. Wymeersch, "Error bounds for uplink and downlink 3d localization in 5g millimeter wave systems," *IEEE Transactions on Wireless Communications*, vol. 17, no. 8, pp. 4939–4954, 2018.

[12] A. Shahmansoori, G. E. Garcia, G. Destino, G. Seco-Granados, and H. Wymeersch, "Position and orientation estimation through millimeter-wave mimo in 5g systems," *IEEE Transactions on Wireless Communications*, vol. 17, no. 3, pp. 1822–1835, 2018.

[13] X. Gao, L. Dai, and A. M. Sayeed, "Low RF-Complexity Technologies to Enable Millimeter-Wave MIMO with Large Antenna Array for 5G Wireless Communications," *IEEE Communications Magazine*, vol. 56, no. 4, pp. 211–217, 2018.

[14] J.-N. Shim, H. Park, C.-B. Chae, D. K. Kim, and Y. C. Eldar, "Cramér–Rao Lower Bound on AoA Estimation Using an RF Lens-Embedded Antenna Array," *IEEE Antennas and Wireless Propagation Letters*, vol. 17, no. 12, pp. 2359–2363, 2018.

[15] S. M. Kay, *Fundamentals of statistical signal processing: estimation theory*. Prentice-Hall, Inc., 1993.

[16] L. Yang, Y. Zeng, and R. Zhang, "In-band wireless information and power transfer with lens antenna array," *IEEE Communications Letters*, vol. 21, no. 1, pp. 100–103, 2017.

[17] F. A. Jenkins and H. E. White, "Fundamentals of optics," *New York: McGraw-Hill*, 1957.

[18] Q. C. Li, G. Wu, and T. S. Rappaport, "Channel model for millimeter-wave communications based on geometry statistics," in *2014 IEEE Globecom Workshops (GC Wkshps)*, 2014, pp. 427–432.